Time-Resolved Fluorescence Study on Liquid Oligo(ethylene oxide)s: Coumarin 153 in Poly(ethylene glycol)s and Crown Ethers

Hideaki Shirota* and Hiroshi Segawa

Department of General Systems Sciences, Graduate School of Arts and Sciences, University of Tokyo, 3-8-1 Komaba, Meguro-ku, Tokyo 153-8902, Japan

Received: December 3, 2002

We have investigated the solvation dynamics and reorientation of coumarin 153 (C153) in liquid poly(ethylene glycol)s with molecular weights of 150, 194, 238, 300, 400, and 600 and liquid crown ethers 12-crown-4 and 15-crown-5 using picosecond time-resolved emission spectroscopy. The observed subnanosecond solvation dynamics is characterized by a biexponential function. The faster solvation time constant is about 130 ps, and this time constant is insensitive to the molecular weight and the molecular geometric structures. The time constant for slower solvation dynamics (0.5−1.6 ns range) varies with the change of the molecular weight and the different molecular geometric structures of the macromolecules. The features of the orientational dynamics of C153 in poly(ethylene glycol)s and crown ethers are similar to those of the solvation dynamics. Both the slower solvation and reorientation time constants of coumarin 153 in poly(ethylene glycol)s are linearly correlated with the bulk viscosity.

1. Introduction

Solvation dynamics have been well studied to characterize the ultrafast dynamical aspects in solutions, because the solvation dynamics is an important factor to control the reaction, ionic mobility, and transportation of a molecule in solutions.[1−5] The normalized solvation time correlation function is expressed by

$$S(t) = \frac{E_{sol}(t) - E_{sol}(\infty)}{E_{sol}(0) - E_{sol}(\infty)} \quad (1)$$

where $E_{sol}(t)$, $E_{sol}(0)$, and $E_{sol}(\infty)$ are the solvation energies of a solute at times t, 0, and ∞. Maroncelli and co-workers summarized the solvation times for 24 typical organic solvents studied by dynamic fluorescence Stokes shift measurements.[6]

Studies on the solvation dynamics have now extended to the complex condensed phases, such as micelles,[7−9] aqueous[10−15] and nonaqueous[16−18] reverse micelles, vesicles,[19,20] a Langmuir layer,[21] cyclodexitrines,[22−24] proteins,[25−27] DNA,[28] nonideal binary solutions,[29−35] glasses,[36−38] and interfaces of liquid inorganic materials.[39−41] Since these complex condensed phases are largely inhomogeneous, the intermolecular interactions, orientations of the medium molecules, and intramolecular conformations are complicated in comparison with those of the simple solutions. As a result, the dynamical features in complex condensed phases are very much different from those in simple solutions. Current progress in this area is reviewed by Bhattacharrya et al.,[42] Levinger,[43] and Richert.[38d]

The dynamical features of polymer liquids and polymer solutions are very complex, because the broad time range polymer dynamics consists of the local (constitutional repeat units, segments, and side groups) motions, entire polymer motion, and cooperative motions. Since the fluorescence Stokes shift measurement is a very useful method to investigate the dynamical feature of the complex condensed phase, several studies on the solvation dynamics in polymer systems were also reported. Bhattacharyya and co-workers studied the solvation dynamics in aqueous polyacrylamide gel[44] and aqueous poly(vinylpyrrolidone) solution[45] by using picosecond laser spectroscopy. They found that the solvation dynamics in aqueous polyacrylamide gel was undetectable by a picosecond instrument with a temporal response of 50 ps (this means that the solvation dynamics quickly occurs much faster than 50 ps) but the nanosecond solvation dynamics was resolved in aqueous poly(vinylpyrrolidone) solution. In agreement with their result, we found recently that the diffusive local dynamics in aqueous polyacrylamide solutions with a bulk viscosity of hundreds of centipoise occurs within the time of 10 ps.[46] Castner and co-wokers reported that the solvation dynamics in aqueous poly(ethylene oxide) (PEO)[8,47] and amphiphilic starlike macromolecule, which is comprised mostly of PEO,[8] solutions. The solvation dynamics in aqueous PEO solution occurs on a broad time scale (1 ps to 4 ns).

In this study, we have investigated the solvation dynamics in liquid poly(ethylene glycol)s (PEGs) with molecular weights of 150, 194, 238, 300, 400, and 600 and crown ethers (CEs) 12-crown-4 and 15-crown-5 using picosecond time-resolved emission spectroscopy. Since PEGs, the oligomers of PEOs, have no side groups, they are good compounds to investigate the molecular weight dependence on the fast dynamics arising from the main chain (no contribution from the side groups). Further, it is interesting to see the geometric molecular shape effect on the dynamics from the comparison between linear and cyclic oligomers. The oligomer dynamics are of importance not only from the standpoint of a fundamental interest in the molecular liquid and polymer liquid, but also because of their contribution to, or even control of, the properties of ion transportation in PEO, which is of interest for use as an electrolyte support.[48,49] Our main focus points in this study are (i) the molecular weight dependence of PEG on the solvation

* To whom correspondence should be addressed. E-mail: cshirota@mail.ecc.u-tokyo.ac.jp.

10.1021/jp022514l CCC: $25.00
Published on Web 04/18/2003

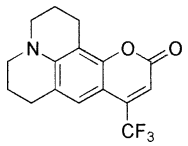

Figure 1. Chemical structure of coumarin 153.

dynamics and (ii) the geometric structure effect on the solvation dynamics (the comparison between PEG and CE).

2. Experimental Section

Laser-grade coumarin 153 (C153; Figure 1) was purchased from Exiton and used without further purification. This fluorescence probe molecule is a typical solvatochromic molecule for the solvation dynamics studies.[6,50,51] Tri(ethylene glycol) (EG3; FW = 150, Aldrich), tetra(ethylene glycol) (EG4; FW = 194, Aldrich), penta(ethylene glycol) (EG5; FW = 238, Aldrich), poly(ethylene glycol)s (M_n = 300 (PEG300; Aldrich), 400 (PEG400; Lancaster), and 600 (PEG600; Aldrich)), 12-crown-4 (CE4; FW = 176, Wako), and 15-crown-5 (CE5; FW = 220, Wako) were also used as received. The concentration of C153 in PEO was kept at about 2×10^{-5} M. The steady-state absorption and fluorescence spectra of C153 in PEOs were measured with a JASCO V-570 UV/vis/near-IR spectrometer and a JASCO FP-777 spectrofluorometer, respectively. The viscosities η of the neat PEOs were measured at 295 ± 1 K with a vibrating viscometer (Yamaichi Electronics, VM-1G-L).

A streak camera system was used for the laser spectroscopy. The advantage of this spectroscopic method is that we can directly observe the time-dependent fluorescence spectra, though with a limited time response of about 30 ps. The light source was a femtosecond titanium:sapphire laser (Spectra Physics, Tsunami) at about 800 nm with an average power of approximately 400 mW, pumped by 5.7 W for all-line light of an argon ion laser (Spectra Physics, Beamlok). A combined pulse selector and frequency doubler (Spectra Physics, model 3980) was used to reduce the repetition rate (from 82 to 4 MHz) and to generate the second harmonic light at about 400 nm. The second harmonic light was used to excite the sample, and the remaining fundamental light was used as the trigger signal for a streak camera. The sample was excited by the second harmonic light after passing through a Glan-Laser polarizer to set the vertical polarization angle. The fluorescence of the sample was passed though a 2 mm slit attached to a 10 mm optical-pass-length quartz sample cell, a Glan-Laser polarizer set at the magic, vertical, or horizontal angle to the pump beam, and a polychromator (Jobin Yvon, CP-200), and was detected by a streak camera (Hamamatsu Photonics, C4334). The instrument responses were estimated by the excitation-light scattering of a powdered milk solution in the sample cell. The full widths at half-maximum of the instrument responses were 20−30 ps for the 2 ns full-scale detection, 35−45 ps for 5 ns full-scale detection, 100−130 ps for 10 ns full-scale detection, and 200−250 ps for the 20 ns full-scale detection. All the measurements were made at ambient temperature (296 ± 2 K).

3. Results

3.1. Steady-State Absorption and Fluorescence Spectra and Bulk Viscosity. Figure 2 shows the steady-state absorption and fluorescence spectra of C153 (a) in PEG600, PEG300, and EG3 and (b) in CE5 and CE4. The steady-state absorption and fluorescence spectra of C153 in methanol and cyclohexane are also shown in Figure 1c as references for typical polar and nonpolar solvents. The absorption and fluorescence maxima and Stokes shift ($\Delta\nu = \nu_{abs} - \nu_{fl}$) of C153 in the liquids are summarized in Table 1. The molecular weight M dependence

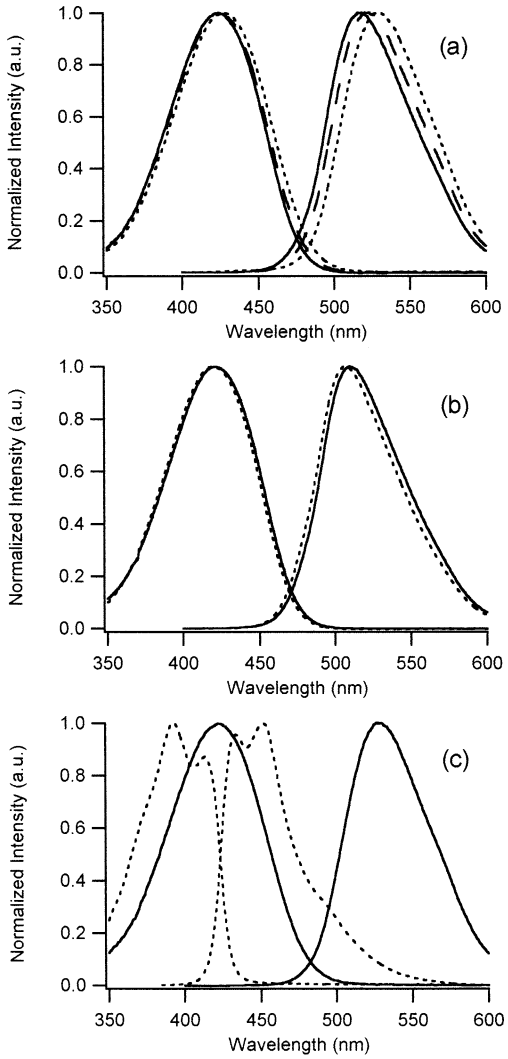

Figure 2. Steady-state absorption and fluorescence spectra of C153 (a) in poly(ethylene glycol)s (solid lines, PEG600; dashed lines, PEG300; dotted lines, EG3), (b) in crown ethers (solid lines, CE5; dotted lines, CE4), and (c) in methanol (solid lines) and cyclohexane (dotted lines).

TABLE 1: Steady-State Absorption and Fluorescence Maxima and Stokes Shifts of C153 in Poly(ethylene glycol)s, Crown Ethers, Methanol, and Cyclohexane and Bulk Viscosities of Poly(ethylene glycol)s, Crown Ethers, Methanol, and Cyclohexane

medium	$\nu_{abs}/10^3$ cm^{-1} (λ_{abs}/nm)	$\nu_{fl}/10^3$ cm^{-1} (λ_{fl}/nm)	$\Delta\nu/10^3$ cm^{-1}	η/cP[a]
EG3	23.41 (427.2)	18.87 (529.9)	4.54	49.1
EG4	23.49 (425.8)	19.00 (526.4)	4.49	60.4
EG5	23.50 (425.5)	19.06 (524.7)	4.44	73.4
PEG300	23.53 (424.9)	19.14 (522.6)	4.39	97.7
PEG400	23.58 (424.1)	19.22 (520.4)	4.36	125
PEG600	23.61 (423.6)	19.31 (517.8)	4.30	171
CE4	23.81 (420.0)	19.71 (507.3)	4.10	12.3
CE5	23.72 (421.5)	19.58 (510.8)	4.14	30.0
methanol	23.68 (422.3)	18.90 (529.0)	4.78	0.544[c,d]
cyclohexane	24.22 (412.9)	23.05 (433.8)	2.24[b]	0.894[c,d]
	25.45 (392.9)	22.14 (451.7)		

[a] The experimental error is ±5%. [b] The value is an average. [c] Values at 298 K. [d] Reference 52.

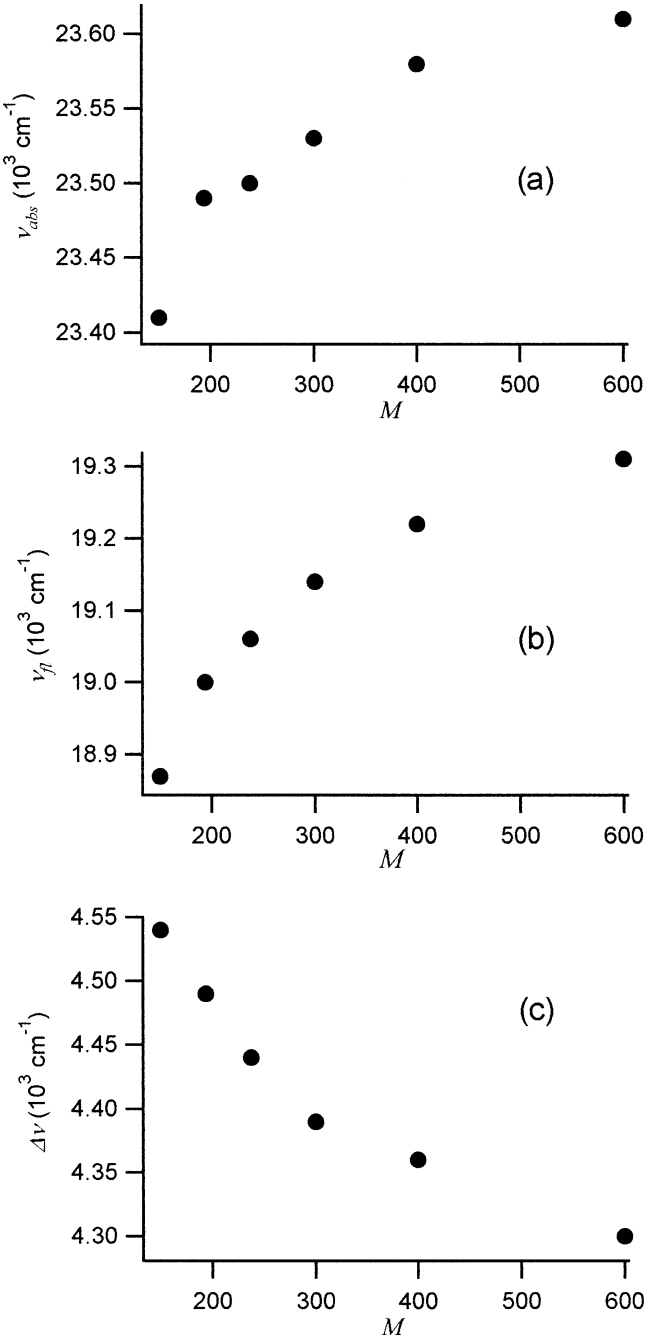

Figure 3. (a) Absorption maxima ν_{abs}, (b) fluorescence maxima ν_{fl}, and (c) Stokes shifts $\Delta\nu$ vs the molecular weight M for C153 in poly(ethylene glycol)s.

of the (a) absorption and (b) fluorescence maximum frequencies and (c) Stokes shift for C153 in PEG is shown in Figure 3. The result shows that both the absorption and fluorescence maxima of C153 in PEG shift to the larger frequencies and the Stokes shift becomes smaller with the larger M of PEG. In contrast to C153 in PEG, both the absorption and fluorescence maximum frequencies of C153 in CE shift to the smaller frequencies and the Stokes shift becomes larger with the larger M of CE.

The bulk viscosities η of the PEGs and CEs measured are listed in Table 1, along with the values of η of methanol and cyclohexane.[52] The η dependence on the molecular weight M of PEG is plotted in Figure 4. It is evident from the viscosity data that (i) η increases with the larger M of the polymer, (ii) the values of η for PEGs are larger than those of CEs which

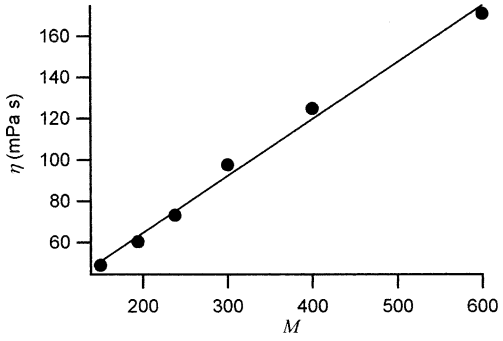

Figure 4. Bulk viscosities η vs molecular weights M for poly(ethylene glycol)s.

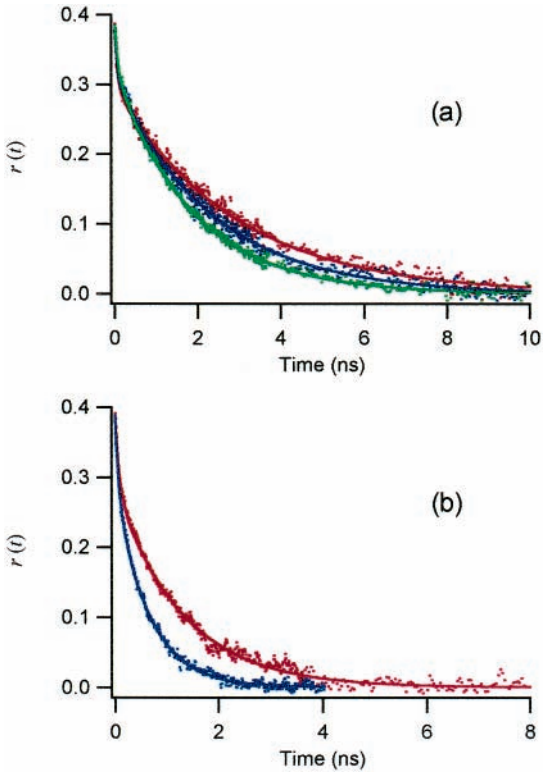

Figure 5. Fluorescence anisotropy decays $r(t)$ for C153 (a) in poly(ethylene glycol)s (red dots, PEG600; blue dots, PEG300; green dots, EG3) and (b) in crown ethers (red dots, CE5; blue dots, CE4). Biexponential fit curves are also shown by the corresponding colored lines.

have the same numbers of the constitutional repeat unit, and (iii) the η of PEG is almost linearly dependent on the M of the polymer.

The bulk viscosity dependence on the molecular weight for polymer melts is empirically expressed as[53−56]

$$\eta(M) = \begin{cases} \eta(M_c)\,(M/M_c) & \text{for } M < M_c \\ \eta(M_c)\,(M/M_c)^{3.4} & \text{for } M > M_c \end{cases} \qquad (2)$$

where M_c is a certain critical molecular weight related to the onset of polymer chain entaglements. PEG also follows the relationship between viscosity and molecular weight. The value of M_c of PEG is about 4400.[56] Because the molecular weights of all the PEGs used in this study are smaller than M_c, the approximately linear scaling observed appears with the previous results.[56]

3.2. Fluorescence Anisotropy Decay. Figure 5 shows the fluorescence anisotropy decays, $r(t)$, for C153 (a) in PEG600,

TABLE 2: Reorientation Parameters for C153 in Poly(ethylene glycol)s and Crown Ethers

medium	a_{r1} ($a_{r1}/(a_{r1}+a_{r2})$)	τ_{r1}/ns	a_{r2} ($a_{r1}/(a_{r1}+a_{r2})$)	τ_{r2}/ns
EG3	0.07 ± 0.01 (0.18)	0.082 ± 0.08	0.32 ± 0.01 (0.82)	1.89 ± 0.02
EG4	0.09 ± 0.01 (0.23)	0.079 ± 0.06	0.30 ± 0.01 (0.77)	2.10 ± 0.03
EG5	0.08 ± 0.01 (0.21)	0.079 ± 0.08	0.30 ± 0.01 (0.79)	2.08 ± 0.05
PEG300	0.08 ± 0.01 (0.21)	0.058 ± 0.10	0.31 ± 0.01 (0.79)	2.34 ± 0.04
PEG400	0.08 ± 0.01 (0.21)	0.058 ± 0.09	0.30 ± 0.01 (0.79)	2.42 ± 0.04
PEG600	0.09 ± 0.01 (0.24)	0.068 ± 0.07	0.29 ± 0.01 (0.76)	2.89 ± 0.05
CE4	0.10 ± 0.01 (0.26)	0.066 ± 0.05	0.29 ± 0.01 (0.74)	0.64 ± 0.03
CE5	0.10 ± 0.01 (0.26)	0.077 ± 0.07	0.29 ± 0.01 (0.74)	1.29 ± 0.04

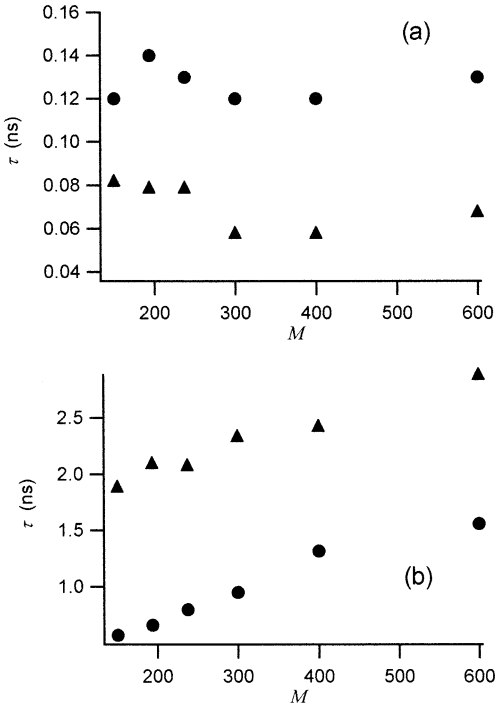

Figure 6. (a) Faster reorientational time constants τ_{r1} (triangles) and faster solvation time constants τ_{s1} (circles) and (b) slower reorientational time constants τ_{r2} (triangles) and slower solvation time constants τ_{s2} (circles) of C153 in poly(ethylene glycol)s vs the molecular weights M of poly(ethylene glycol)s.

PEG300, and EG3 and (b) in CE5 and CE4. $r(t)$ is given by

$$r(t) = \frac{I_{\parallel}(t) - I_{\perp}(t)}{I_{\parallel}(t) + 2I_{\perp}(t)} \tag{3}$$

where $I_{\parallel}(t)$ and $I_{\perp}(t)$ are the tail-matched fluorescence transients polarized parallel and perpendicular to the excitation laser light. The $r(t)$ of C153 in PEG at the time range of 0−0.2 ns is almost independent of the M of PEG, but the $r(t)$ becomes slower with increasing M of PEG. A biexponential function is used to fit the fluorescence anisotropy decays since a single-exponential function does not fit the data. The amplitudes, a_{r1} and a_{r2}, and reorientation times, τ_{r1} and τ_{r2}, are listed in Table 2. All the values of $a_{r1} + a_{r2}$ for C153 in PEGs are close to 0.4 (Table 2), as is the case for simple solvents.[57]

The dependence of PEG's M on the reorientation time constants of C153 in PEG is shown in Figure 6. The slower reorientation time constant τ_{r2} increases with the PEG's M, although the faster rotational diffusion time τ_{r1} is insensitive to the M of PEG within experimental error. The feature of the orientational dynamics of C153 in CE is similar to that in PEG: τ_{r1} values in CE4 and CE5 are almost identical, but τ_{r2} values in CE5 are larger than those in CE4 (Table 2).

3.3. Dynamic Fluorescence Stokes Shift. When a fluorescence probe, which shows a linear relationship between the fluorescence maximum frequency of the fluorescence probe and the solvent polarity, is used to study the solvation process, we can estimate the $S(t)$ from the direct measurement of the dynamic fluorescence Stokes shift of the fluorescence probe. Equation 1 can thus be rewritten as

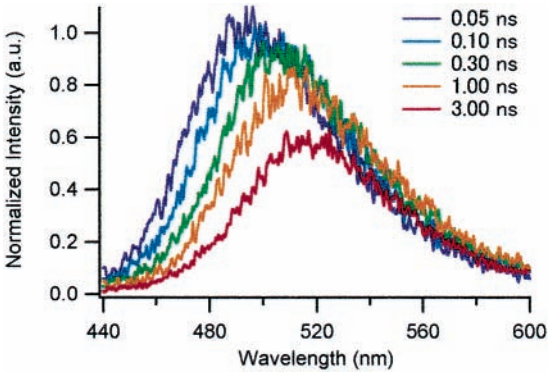

Figure 7. Examples of the time-resolved fluorescence spectra of C153 in PEG600. The fluorescence maximum shifts to the longer wavelength with the time evolution (purple, 0.05 ns; blue, 0.10 ns; green, 0.30 ns; orange, 1.00 ns; red, 3.00 ns).

$$S(t) = \frac{\nu(t) - \nu(\infty)}{\nu(0) - \nu(\infty)} \tag{4}$$

where $\nu(t)$, $\nu(\infty)$, and $\nu(0)$ are the fluorescence maximum frequencies of the fluorescence probe at times t, ∞, and 0, respectively. Time 0 is defined as the time when the dipole moment of the solute changes due to the excitation of the electronic state by light, and time ∞ is defined as the time when the system achieves the equilibrium state. Since the solvation process in most simple solvents is much faster than the lifetime of the fluorescence probe, $\nu(\infty)$ is often defined as the maximum frequency of the steady-state fluorescence spectra. Namely, the dynamic fluorescence Stokes shift of a solvatochromic molecule corresponds to the solvation dynamics.

Figure 7 shows the typical examples of the time-resolved fluorescence spectra of C153 in PEG600 at times of 0.05, 0.10, 0.30, 1.00, and 3.00 ns. It is evident from Figure 7 that the fluorescence maximum shifts to the longer wavelength with the time evolution up to the nanosecond region. The liquid oligo(ethylene oxide)s studied here show the subnanosecond solvation component as well as the other complex solutions,[42,43] though the subnanosecond solvation dynamics is not commonly observed in most of the simple organic solvents.[6] To estimate the maximum of the time-resolved fluorescence spectrum at each time, the time-resolved fluorescence spectra measured are fitted with a log-normal line-shape function:[58]

$$I_f(\nu) = I_{f0} \exp\left[-\ln(2)\left(\frac{\ln[1 + 2b(\nu - \nu_p)/\Delta]}{b}\right)^2\right] \tag{5}$$

where I_{f0}, ν_p, b, and Δ are the peak height, peak frequency,

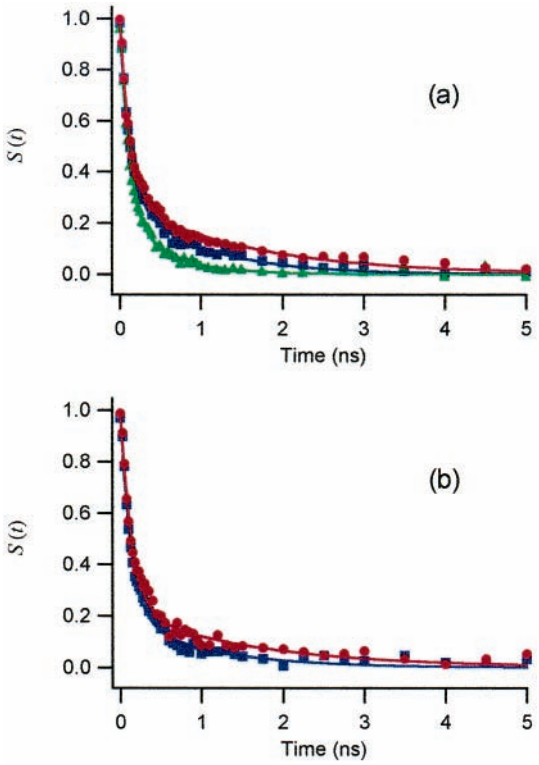

Figure 8. Decays of solvation correlation functions $S(t)$ for C153 (a) in poly(ethylene glycol)s (red circles, PEG600; blue squares, PEG300; green triangles, EG3) and (b) in crown ethers (red circles, CE5; blue squares, CE4). Biexponential fit curves are also shown by the corresponding colored lines.

TABLE 3: Parameters for the Solvation Dynamics of C153 in Poly(ethylene glycol)s and Crown Ethers

medium	a_{s1}	τ_{s1}/ns	a_{s2}	τ_{s2}/ns
EG3	0.78 ± 0.06	0.12 ± 0.01	0.22 ± 0.06	0.57 ± 0.11
EG4	0.79 ± 0.06	0.14 ± 0.02	0.21 ± 0.06	0.66 ± 0.13
EG5	0.70 ± 0.05	0.13 ± 0.01	0.30 ± 0.05	0.80 ± 0.10
PEG300	0.70 ± 0.03	0.12 ± 0.01	0.30 ± 0.03	0.95 ± 0.09
PEG400	0.69 ± 0.02	0.12 ± 0.01	0.31 ± 0.02	1.30 ± 0.10
PEG600	0.70 ± 0.02	0.13 ± 0.01	0.30 ± 0.02	1.56 ± 0.17
CE4	0.80 ± 0.04	0.13 ± 0.01	0.20 ± 0.04	1.02 ± 0.20
CE5	0.78 ± 0.03	0.14 ± 0.01	0.22 ± 0.03	1.62 ± 0.18

asymmetric parameter, and width parameter, respectively. When $2b(\nu - \nu_p)/\Delta$ is less than -1, $I_f(\nu)$ is taken as 0.

The dynamic features of the solvation process of C153 in the oligo(ethylene oxide)s can be expressed by eq 4. For the data analysis, $\nu(0)$ is defined as the maximum frequency of the fluorescence spectrum at the time when a sample is excited by a laser pulse. The value of $\nu(\infty)$ is tentatively estimated from the extrapolation of the biexponential fit to $\nu(t)$ at infinite time,[32] because the slower solvation component (τ_{s2}) is rather competitive with the fluorescence lifetime of C153 in PEGs (about 5 ns). The value of $\nu(\infty)$ estimated by the above method is in good agreement with the maximum frequency of the fluorescence spectrum at >5 ns within experimental error.

Figure 8 shows the decays of $S(t)$ for C153 (a) in PEG600, PEG300, and EG3 and (b) in CE5 and CE4. The biexponential fit curves are also shown in Figure 8. The amplitudes are set to be 1 ($a_{s1} + a_{s2} = 1$) for a convenient normalization. The fit parameters of the solvation dynamics are summarized in Table 3. We also used the sum of a stretched exponential and single-exponential functions ($a_{s1} \exp(-t/\tau_{s1})^{\beta} + a_{s2} \exp(-t/\tau_{s2})$), which is well used to express the polymer dynamics, for the fit to the experimental data. The index β in the stretched exponential function obtained by the fit to $S(t)$ for all the oligo(ethylene oxide)s is almost unity ($0.9 < \beta < 1.1$), and both the amplitudes and time constants are quite similar to those obtained by a biexponential fit function.

To clearly see the dependence of PEG's M on the solvation time constants for C153 in PEG, the plots of the (a) faster solvation time τ_{s1} and (b) slower solvation time τ_{s2} against the M of PEGs are shown in Figure 6. The notable points from Figures 6 and 8 and Table 3 are the following: (i) The slow subnanosecond to nanosecond solvation dynamics are observed for all the PEOs measured in this study. (ii) The faster solvation time constant τ_{s1} in both PEGs and CEs is about 130 ps and is almost independent of the molecular weight and molecular structure (linear or cyclic shape). (iii) The slower solvation time constant τ_{s2} in both PEG and CE becomes slower with the larger M of the molecules. (iv) The slower solvation time constant τ_{s2} in PEGs depends linearly on the M of the polymers.

4. Discussion

4.1. Steady-State Absorption and Fluorescence Spectra. As shown in Figure 3, both the ν_{abs} and ν_{fl} of C153 in PEGs become larger and $\Delta\nu$ becomes smaller with the larger M of PEG. However, the relationships between ν_{abs}, ν_{fl}, and $\Delta\nu$ and the M of PEG for C153 in PEG are not simple. We rescale from M to the volume fraction of the hydroxyl groups of the entire polymer, $V_{OH}/V_{molecule}$, because PEG has two polar hydroxyl groups per molecule and the ethylene oxide main chain is much less polar than the hydroxyl end group.

Figure 9 shows the dependence of the ν_{abs}, ν_{fl}, and $\Delta\nu$ of C153 in PEG on $V_{OH}/V_{molecule}$. The volumes of the hydroxyl group and polymer are estimated from the sum of the van der Waals increments.[59] Interestingly, all the ν_{abs}, ν_{fl}, and $\Delta\nu$ values of C153 in PEG depend linearly on $V_{OH}/V_{molecule}$. This indicates that the static solvation energy (or the solvent reorganization energy λ_s) of C153 in PEG depends linearly on the volume fraction of the polar group in the molecule, because λ_s can be estimated by the fluorescence Stokes shifts in the target solvent and in a nonpolar solvent as the reference:[60]

$$\lambda_s = (\Delta\nu - \Delta\nu_{ref})/2 \qquad (6)$$

where $\Delta\nu$ and $\Delta\nu_{ref}$ are the Stokes shifts in the target solvent and in the reference nonpolar solvent, respectively. Since $\Delta\nu_{ref}$ is a constant, λ_s is directly correlated with $\Delta\nu$. Namely, the hydroxyl groups of PEG have a contribution to the stabilization of the excited-state C153 in PEG systems, and the volume fraction of the hydroxyl group is linearly related to a static solvation parameter.

4.2. Orientational Dynamics of C153. The reorientational time correlation function $r(t)$ for C153 in PEG and CE is expressed by a biexponential function as shown in Figure 5. Nonexponential behaviors of the orientational dynamics of C153 in alcohols and some organic solvents were also reported.[57] The notable point of the present result is that the faster reorientation time constant τ_{r1} is about 70 ps for all the PEGs and the slower reorientation time constant τ_{r2} with a time range of 1.8−3.0 ns shows a linear relationship with the M of PEG in the range of $M = 150-600$.

The orientational dynamics of both solvent and solute molecules in simple solutions follows the hydrodynamic models.[61,62] In a simple hydrodynamic model, the rotational diffusion

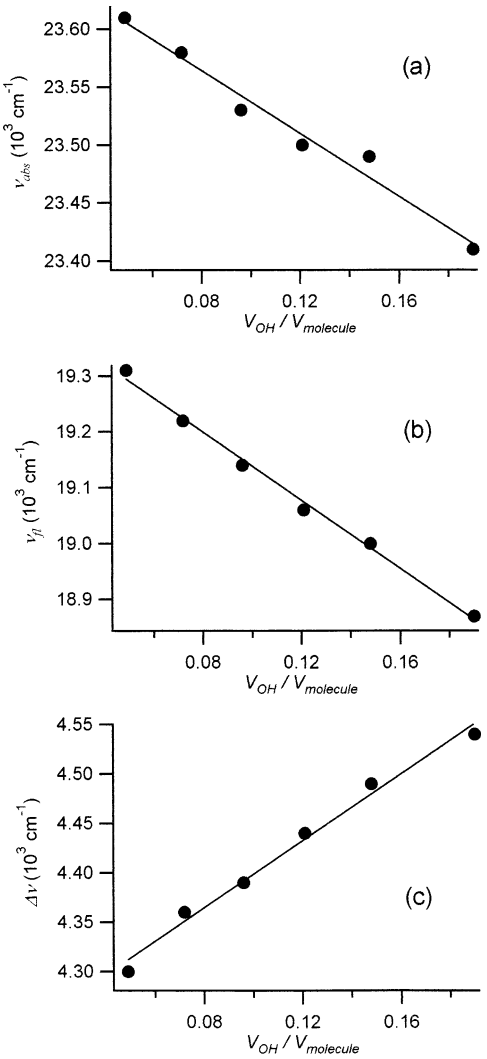

Figure 9. Dependence of the frequencies of the (a) absorption maximum ν_{abs}, (b) fluorescence maximum ν_{fl}, and (c) Stokes shift $\Delta\nu$ of C153 in poly(ethylene glycol) on the volume fraction of the polar hydroxyl group, $V_{OH}/V_{molecule}$.

time of a spherical particle, τ_r, is expressed by

$$\tau_r = \frac{3V\eta fC}{k_B T} + \tau_{r0} \qquad (7)$$

where V is the volume of the target particle, η is the medium viscosity, k_B is the Boltzmann constant, T is the absolute temperature, f is the shape factor, C is the solute−medium coupling friction factor, and τ_{r0} is the free-rotator correlation time. Sluch et al. reported that the rotational time constant of anthracene in poly(isobutylene) with a molecular weight of less than 560 (η is 1300 cP for $M = 560$) obeys the hydrodynamics model and the model breaks down in the larger M poly(isobutylene).[63]

From Figures 4 and 6b, we find a nearly linear dependence of the τ_{r2} of C153 in PEG on the η for the liquid polymers. Since we used only the C153 probe in this study, V and f in eq 7 are invariable parameters. Coumarin derivatives make specific hydrogen bonds with hydrogen-bonding solvent molecules.[64−66] The parameter C varies for polymers with different M values, because the mole fraction (or volume fraction) of hydroxyl groups in the polymer decreases with the larger M of PEG. However, the volume fraction of hydroxyl groups in PEG is not linear to M (and η) (Figures 4 and 9). Therefore, the specific interaction between C153 and hydroxyl groups of PEG could not (or only slightly) vary C with the PEGs with different M values. As a result, the slower orientational dynamics of C153 in PEGs obeys the hydrodynamic model. In contrast to the slower reorientation, the faster reorientation occurs very rapidly like low-viscosity solvents and is insensitive to the PEG chain length and molecular structure. Since the densities of PEGs and CEs are not much different (the densities of EG3, PEG600, CE4, and CE5 are 1.125, 1.128, 1.089, and 1.109 g/mL, respectively) and they have the same constitutional repeat unit, we can expect that the free volume in the liquids might be nearly constant. The present result of the faster reorientation of C153 in PEGs and CEs may arise from no difference of the free volumes of the liquids.

4.3. Solvation Dynamics in Oligo(ethylene oxide)s. Any simple solvent has the ultrafast solvation component in the femtosecond region.[6] When an apparatus whose instrument response is insufficient to resolve the solvation dynamics is used, the observation of the dark solvation component, which is undetectable with the apparatus, is well recognized in pure solvents[67] and micelle solutions.[13,17] Since the instrument response of the spectrometer used in this study is about 30 ps in the shortest detection condition, we need to determine the whole solvation process of C153 in PEGs and CEs we have observed in this study.

The maximum frequency of the time-zero fluorescence spectra of C153 in PEO can roughly be estimated by the method proposed by Fee and Maroncelli.[67] The time-zero spectrum here means a fluorescence spectrum prior to any solvent relaxation. It is not the experimental time-zero fluorescence spectrum. The time-zero frequency of the fluorescence spectrum maximum can be estimated from the steady-state absorption and fluorescence spectra in nonpolar solvent and the absorption spectrum in the target polar solvent:

$$\nu_{p,fmd}(t = 0) = \nu_{p,amd} - [\nu_{np,amd} - \nu_{np,fmd}] \qquad (8)$$

where the subscripts "p" and "np" refer to the spectra in polar and nonpolar solvents. The frequencies here are not the values of the maximum frequencies but correspond to the midpoint frequencies of absorption or fluorescence spectra, ν_{amd} or ν_{fmd}, in the solvents. The midpoint frequency is given by

$$\nu_{md} = (\nu_l + \nu_h)/2 \qquad (9)$$

where ν_l and ν_h are the low and high frequencies (red and blue wavelengths) on the half-height points of the spectrum. Cyclohexane is used as the reference of the nonpolar solvent in the present work. The maximum frequency at time zero, $\nu_{p,f}(t = 0)$, is estimated as the sum of $\nu_{p,fmd}(t = 0)$ and the difference between the midpoint and maximum frequencies in the steady-state fluorescence spectrum of the target system. The calculated time-zero wavelengths of the fluorescence spectra of C153 in PEGs and CEs, $\nu_{cal}(0)$, are listed in Table 4. The maximum frequencies of the observed time-resolved fluorescence spectra of C153 in the oligo(ethylene oxide)s, $\nu(0)$, the maximum frequencies of the fluorescence spectra at infinite time, $\nu(\infty)$, and the dark solvation components $((\nu_{cal}(0) - \nu(0))/(\nu_{cal}(0) - \nu(\infty)))$, which are undetectable with the present laser setup, are also listed in Table 4. The solvation dynamics of C153 in PEGs and CEs discussed here contribute about 60% to the whole solvation process for the PEGs and about 50% for the CEs.

In this study, we observed that τ_{s1} is about 130 ps for all the PEGs and CEs measured, but τ_{s2} becomes slower with the larger M of the molecule. Pant and Levinger recently measured the

TABLE 4: Calculated Time-Zero Fluorescence Maxima $\nu_{cal}(0)$, Observed Time-Zero Fluorescence Maxima $\nu(0)$, Infinite-Time Fluorescence Maxima $\nu(\infty)$, and Dark Solvation Components of C153 in Poly(ethylene glycol)s and Crown Ethers

medium	$\nu_{cal}(0)/10^3$ cm^{-1} ($\lambda_{cal}(0)$/nm)	$\nu(0)/10^3$ cm^{-1} ($\lambda(0)$/nm)	$\nu(\infty)/10^3$ cm^{-1} ($\lambda(\infty)$/nm)	dark solvation component[a]
EG3	20.71 (482.9)	19.90 (502.6)	18.83 (531.1)	0.43
EG4	20.83 (480.0)	20.02 (499.5)	18.93 (528.3)	0.43
EG5	20.85 (479.6)	20.14 (496.5)	18.99 (526.6)	0.38
PEG300	20.92 (478.1)	20.24 (494.0)	19.06 (524.5)	0.37
PEG400	20.95 (477.3)	20.32 (492.2)	19.12 (523.1)	0.34
PEG600	20.96 (477.0)	20.28 (493.2)	19.20 (520.8)	0.39
CE4	21.24 (470.8)	20.43 (489.6)	19.67 (508.5)	0.52
CE5	21.15 (472.8)	20.32 (492.1)	19.52 (512.3)	0.51

[a] Calculated as $(\nu_{cal}(0) - \nu(0))/(\nu_{cal}(0) - \nu(\infty))$.

solvation dynamics of coumarin 343, which is similar to C153, in tri(ethylene glycol) monoethyl ether by femtosecond laser spectroscopy.[12e] They found that the solvation dynamics in tri(ethylene glycol) monoethyl ether is expressed by a triexponential function with time constants of 0.26, 24, and 105 ps (the amplitudes are 0.10, 0.19, and 0.71, respectively). Argaman and Huppert reported the solvation dynamics in di(ethylene glycol) dimethyl ether, tri(ethylene glycol) dimethyl ether, and tetra(ethylene glycol) dimethyl ether.[68] According to their result, the ~10 ps solvation component, which is attributed to the intramolecular segmental motion, depends on the molecular weight (i.e., the longer the polymer, the slower the solvation time constant) and the ~100 ps solvation component, which is related to cooperative motions of the polymer molecules due to the creation and annihilation of the network by the fluctuations, is almost insensitive to the M of the polymers. This result is in good agreement with the results of the Brillouin scattering measurements,[69−72] dielectric measurements,[73,74] and molecular dynamics simulations.[75] Our result also shows no dependence of PEG's M on the ~100 ps dynamics in an even wider molecular weight range ($150 < M < 600$). Further, we find that cyclic CEs also have a ~100 ps solvation component, and this component is almost unity for both CE4 and CE5. That is, the ~100 ps solvation component in PEGs and CEs is related to cooperative motions arising from the local dynamics of ethylene oxide parts of PEGs and CEs and has no relevance to the chain length, end groups, and molecular geometric structures.

In contrast to the 130 ps component of the solvation dynamics, the slower time constant for the solvation dynamics depends on the M of PEGs and is about 10% of the total amplitude of the solvation process. Since η is an important physical parameter for the dynamics in liquids[1−5,61,62] and polymer solutions,[54−56,76,77] we consider the relationship between the time constant of the slower solvation dynamics and the bulk viscosity. It is clear from Figures 4 and 9 that τ_{s2} and η for C153 in PEG have a nearly linear correlation.

As shown from the dependence of η on the M for PEG (Figure 4), the PEGs used in this study are not entangled.[53−56] Further, the slower orientational dynamics of C153 in PEGs obeys the hydrodynamic model. If the slower solvation dynamics is due to the reorientation of the entire oligomer molecule, the slower solvation time constant should be in accord with the hydrodynamic model (eq 7). The correlation between the PEG's volume[59] and M is also linear. However, if both η and M are taken into consideration, the change of the time constants is too small. It is thus less possibile that the linear PEG behaves as a small rigid particle (the Stokes−Einstein−Debye hydrodynamic model).

It is known that the *longest* rotational relaxation time of a polymer can be expressed by the Rouse model in some cases

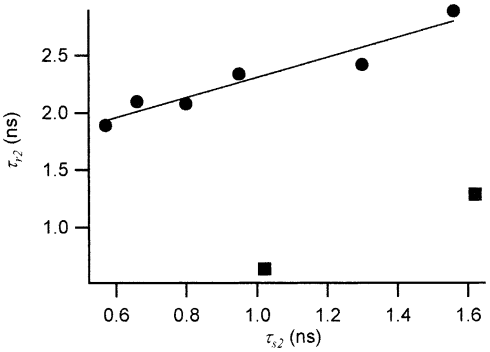

Figure 10. Slower reorientation time constants τ_{r2} vs the slower solvation time constants τ_{s2} for C153 in poly(ethylene glycol)s (circles) and in crown ethers (squares). τ_{r2} depends linearly on τ_{s2} for C153 in poly(ethylene glycol)s.

of short polymers (oligomers) in melts.[78] According to the Rouse model, the diffusion constant D is proportional to $1/M$ and the time constant of the relaxation is proportional to the square of M.[54−56,79] Shi and Vincent reported the molecular weight dependence of PEO on lithium cation mobility in PEO.[80] They showed that the mobility of the cation in low molecular weight PEOs (below the entanglement limit) was explained by the Rouse−Zimm model. Borodian and Smith estimated the Rouse time of PEO with $M = 530$ at 450 and 363 K by the molecular dynamics simulation.[81] The time constant is in good agreement with the present result (τ_{s2} for PEGs with $M = 400$ and 600). However, the present result shows the linear dependence of τ_{s2} on M. Interestingly, only the smallest molecular weight PEO studied by Shi and Vincent ($M = 400$) showed an anomalously high value of the diffusion coefficient D of the lithium cation for the feature of the Rouse model ($D \propto M^{-\sim 2}$).[80] Since the molecular weight range in the present experiment is much lower than in Shi and Vincent's experiment ($400 < M < 3200$, the Rouse region), the mechanism of the observed oligomer dynamics may be different from that of the Rouse model.

The slow nanosecond solvation dynamics is also observed in CEs. From the comparison between the time constants of the slower solvation dynamics in CEs and PEGs which have the same numbers of the constitutional repeat unit, it is evident that the slower solvation dynamics in CEs is slower than that in PEGs, though the values of η of CEs are smaller than those of PEGs. Further, the time constants of the slower orientational dynamics in the CEs are larger than those of the slower solvation dynamics in the PEGs with the same numbers of the constitutional repeat units, though the time constants of the slower orientation dynamics in the PEGs are smaller than those of the slower solvation dynamics in the CEs.

In simple solutions, there is a correlation between the orientational dynamics and the diffusive solvation dynamics.[57,82] Figure 10 shows the plots of τ_{r2} vs τ_{s2} for C153 in PEGs (circles) and in CEs (squares). It is clear from Figure 10 that the correlation between τ_{r2} and τ_{s2} for C153 in PEGs is also linear. Moreover, we find the correlation for PEG is different from that of CE. Similarly to the present result, Maroncelli and coworkers showed that the correlation between the orientational dynamics and the solvation dynamics for C153 in linear alcohols is different from that for C153 in polar aprotic solvents.[57] Although the PEGs and CEs studied here are oligomer systems, not simple solution systems, the different features of PEG and CE might arise from the presence of hydrogen-bonding sources as in the case of simple solution systems.

5. Conclusions

The solvation dynamics and orientational dynamics of a solvatochromic fluorescence probe molecule, coumarin 153, in liquid poly(ethylene glycol)s and crown ethers have been investigated by picosecond time-resolved emission spectroscopy. The time constant of the faster solvation dynamics in poly(ethylene glycol) is ~130 ps and does not depend on the molecular weight in the range of $M = 150-600$. In contrast to the faster solvation time constant, the time constant of the slower solvation dynamics (0.5−1.6 ns) depends linearly on the molecular weight and bulk viscosity of poly(ethylene glycol). The feature of the orientational dynamics of C153 in liquid poly(ethylene glycol)s is similar to that of the solvation dynamics: the faster reorientational time is almost constant (~70 ps), and the slower reorientational time constant (1.8−3.0 ns) depends linearly on the molecular weight and bulk viscosity of poly(ethylene glycol). From the comparison between poly(ethylene glycol) and crown ether, we found that the faster solvation dynamics in crown ethers is similar to that in poly(ethylene glycol)s. However, the slower solvation dynamics in crown ethers is somewhat different from that in poly(ethylene glycol)s. This difference between crown ether and poly(ethylene glycol) is due to the distinction of the molecular structures including the presence of hydroxyl groups.

Acknowledgment. We are grateful to Prof. Kankan Bhattacharyya (Indian Association for the Cultivation of Science) and Prof. Edward W. Castner, Jr. (Rutgers University) for fruitful discussions. We also thank Prof. Edward W. Castner, Jr. and Mr. Yushi Tamoto (University of Tokyo) for their critical reading of this manuscript. This work is partially supported by the Yamada Science Foundation and the Sasakawa Scientific Research Grant from the Japan Science Society (H. Shirota). We also acknowledge the Ministry of Education, Culture, Sports, Science and Technology of Japan (Grant-in-Aid for Scientific Research on Priority Areas 417).

References and Notes

(1) Barbara, P. F.; Jarzeba, W. *Adv. Photochem.* **1990**, *15*, 1.
(2) Maroncelli, M. *J. Mol. Liq.* **1993**, *57*, 1.
(3) Fleming, G. R.; Cho, M. *Annu. Rev. Phys. Chem.* **1996**, *47*, 109.
(4) de Boeji, W. P.; Pshenikov, M. S.; Wiersma, D. A. *Annu. Rev. Phys. Chem.* **1998**, *49*, 99.
(5) Bagchi, B.; Biswas, R. *Adv. Chem. Phys.* **1999**, *109*, 207.
(6) Horng, M. L.; Gardecki, J. A.; Frankland, S. J. V.; Maroncelli, M. *J. Phys. Chem.* **1995**, *99*, 17311.
(7) (a) Sarkar, N.; Datta, A.; Das, S.; Bhattacharyya, K. *J. Phys. Chem.* **1996**, *100*, 15483. (b) Datta, A.; Mandal, D.; Pal, S. K.; Das, S.; Bhattacharyya, K. *J. Mol. Liq.* **1998**, *77*, 121. (c) Mandal, D.; Sen, S.; Bhattacharyya, K.; Tahara, T. *Chem. Phys. Lett.* **2002**, *359*, 77.
(8) Frauchiger, L.; Shirota, H.; Uhrich, E. K.; Castner, E. W., Jr. *J. Phys. Chem. B* **2002**, *106*, 7463.
(9) (a) Balasubramanian, S.; Bagchi, B. *J. Phys. Chem. B* **2001**, *105*, 12529. (b) Balasubramanian, S.; Bagchi, B. *J. Phys. Chem. B* **2002**, *106*, 3668. (c) Pal, S.; Balasubramanian, S.; Bagchi, B. *J. Chem. Phys.* **2002**, *117*, 2852.
(10) (a) Zhang, J.; Bright, F. V. *J. Phys. Chem.* **1991**, *95*, 7900. (b) Zhang, J.; Bright, F. V. *J. Phys. Chem.* **1992**, *96*, 5633. (c) Zhang, J.; Bright, F. V. *J. Phys. Chem.* **1992**, *96*, 9068. (d) Lundgren, J. S.; Heitz, M. P.; Bright, F. V. *Anal. Chem.* **1995**, *67*, 3775.
(11) (a) Sarkar, N.; Das, K.; Datta, A.; Das, S.; Bhattacharyya, K. *J. Phys. Chem.* **1996**, *100*, 10523. (b) Das, S.; Datta, A.; Bhattacharyya, K. *J. Phys. Chem. A* **1997**, *101*, 3299. (c) Mandal, D.; Datta, A.; Pal, S. K.; Bhattacharyya, K. *J. Phys. Chem. B* **1998**, *102*, 9070. (d) Pal, S. K.; Mandal, D.; Sukul, D.; Bhattacharyya, K. *Chem. Phys. Lett.* **1999**, *312*, 178.
(12) (a) Willard, D. M.; Riter, R. E.; Levinger, N. E. *J. Am. Chem. Soc.* **1998**, *120*, 4151. (b) Riter, R. E.; Undiks, E. P.; Levinger, N. E. *J. Am. Chem. Soc.* **1998**, *120*, 6062. (c) Rant, D.; Riter, R. E.; Levinger, N. E. *J. Chem. Phys.* **1998**, *109*, 9995. (d) Willard, D. M.; Levinger, N. E. *J. Phys. Chem. B* **2000**, *104*, 11075. (e) Pant, D.; Levinger, N. E. *Langmuir* **2000**, *16*, 10123.
(13) Raju, B. B.; Costa, S. M. B. *Phys. Chem. Chem. Phys.* **1999**, *1*, 5029.
(14) (a) Faeder, J.; Ladanyi, B. M. *J. Phys. Chem. B* **2000**, *104*, 1033. (b) Faeder, J.; Ladanyi, B. M. *J. Phys. Chem. B* **2001**, *105*, 11148.
(15) Hazra, P.; Sarkar, N. *Chem. Phys. Lett.* **2001**, *342*, 303.
(16) Riter, R. E.; Undiks, E. P.; Kimmel, J. R.; Levinger, N. E. *J. Phys. Chem. B* **1998**, *102*, 7931.
(17) Shirota, H.; Horie, K. *J. Phys. Chem. B* **1999**, *103*, 1437.
(18) (a) Hazra, P.; Sarkar, N. *Phys. Chem. Chem. Phys.* **2002**, *4*, 1040. (b) Hazra, P.; Chakrabarty, D.; Sarkar, N. *Chem. Phys. Lett.* **2002**, *358*, 523.
(19) (a) Datta, A.; Pal, S. K.; Mandal, D.; Bhattacharyya, K. *J. Phys. Chem. B* **1998**, *102*, 6114. (b) Pal, S. K.; Sukul, D.; Mandal, D.; Bhattacharyya, K. *J. Phys. Chem. B* **2000**, *104*, 4529. (c) Pal, S. K.; Sukul, D.; Mandal, D.; Sen, S.; Bhattacharyya, K. *Tetrahedron* **2000**, *56*, 6999.
(20) Bursing, H.; Ouw, D.; Kundu, S.; Vohringer, P. *Phys. Chem. Chem. Phys.* **2001**, *3*, 2378.
(21) (a) Benderskii, A. V.; Eisenthal, K. B. *J. Phys. Chem. B* **2000**, *104*, 11723. (b) Benderskii, A. V.; Eisenthal, K. B. *J. Phys. Chem. B* **2001**, *105*, 6698. (c) Benderskii, A. V.; Eisenthal, K. B. *J. Phys. Chem. A* **2002**, *106*, 7482.
(22) Vajda, S.; Jimenez, R.; Rosenthal, S. J.; Fidler, V.; Fleming, G. R.; Castner, E. W., Jr. *J. Chem. Soc., Faraday Trans.* **1995**, *91*, 867.
(23) Sen, S.; Sukul, D.; Dutta, P.; Bhattacharyya, K. *J. Phys. Chem. A* **2001**, *105*, 10635.
(24) Nandi, N.; Bagchi, B. *J. Phys. Chem.* **1996**, *100*, 13914.
(25) (a) Joo, T.; Jia, Y.; Yu, J.-Y.; Jonas, D. M.; Fleming, G. R. *J. Phys. Chem.* **1996**, *100*, 2399. (b) Jimenez, R.; Van Mourik, F.; Fleming, G. R. *J. Phys. Chem. B* **1997**, *101*, 7350. (c) Yu, J.-Y.; Nagasawa, Y.; Van Grondelle, R.; Fleming, G. R. *Chem. Phys. Lett.* **1997**, *280*, 404. (d) Groot, M.-L.; Yu, J.-Y.; Agarwal, R.; Norris, J. R.; Fleming, G. R. *J. Phys. Chem. B* **1998**, *102*, 5923. (e) Jordanides, X. J.; Lang, M. J.; Song, X.; Fleming, G. R. *J. Phys. Chem. B* **1999**, *103*, 7995.
(26) Homoelle, B. J.; Edington, M. D.; Diffey, W. M.; Beck, W. F. *J. Phys. Chem. B* **1998**, *102*, 3044.
(27) (a) Zhong, D.; Pal, S. K.; Zewail, A. H. *Chemphyschem* **2001**, *2*, 219. (b) Pal, S. K.; Peon, J.; Zewail, A. H. *Proc. Natl. Acad. Sci. U.S.A.* **2002**, *99*, 1763.
(28) (a) Brauns, E. B.; Madaras, M. L.; Coleman, R. S.; Murphy, C. J.; Berg, M. A. *J. Am. Chem. Soc.* **1999**, *121*, 11644. (b) Brauns, E. B.; Madaras, M. L.; Coleman, R. S.; Murphy, C. J.; Berg, M. A. *Phys. Rev. Lett.* **2002**, *88*, 158101.
(29) Jarzeba, W.; Walker, G. C.; Johnson, A. E.; Barbara, P. F. *Chem. Phys.* **1991**, *152*, 57.
(30) Cichos, F.; Willert, A.; Rempel, U.; von Borczyskowski, C. *J. Phys. Chem. A* **1997**, *101*, 8179.
(31) Gardecki, J. A.; Maroncelli, M. *Chem. Phys. Lett.* **1999**, *301*, 571.
(32) Shirota, H.; Castner, E. W., Jr. *J. Chem. Phys.* **2000**, *112*, 2367.
(33) (a) Chandra, A.; Bagchi, B. *J. Chem. Phys.* **1991**, *94*, 8367. (b) Chandra, A. *Chem. Phys. Lett.* **1995**, *235*, 133.
(34) (a) Day, T. J. F.; Patey, G. N. *J. Chem. Phys.* **1997**, *106*, 2782. (b) Yoshimori, A.; Day, T. J. F.; Patey, G. N. *J. Chem. Phys.* **1998**, *109*, 3222.
(35) (a) Skaf, M. S.; Ladanyi, B. M. *J. Phys. Chem.* **1996**, *100*, 18258. (b) Laria, D.; Skaf, M. S. *J. Chem. Phys.* **1999**, *111*, 300.
(36) (a) Joo, T.; Jia, Y.; Yu, J.-Y.; Lang, M. J.; Fleming, G. R. *J. Chem. Phys.* **1996**, *104*, 6089. (b) Nagasawa, Y.; Passino, S. A.; Joo, T.; Fleming, G. R. *J. Chem. Phys.* **1997**, *106*, 4840. (c) Nagasawa, Y.; Yu, J.-Y.; Fleming, G. R. *J. Chem. Phys.* **1998**, *109*, 6175.
(37) de Silvestri, S.; Weiner, A. M.; Fujimoto, J. G.; Ippen, E. P. *Chem. Phys. Lett.* **1997**, *280*, 127.
(38) (a) Streck, C.; Mel'nichenko, B.; Richert, R. *Phys. Rev. B* **1996**, *53*, 5341. (b) Wendt, H.; Richert, R. *J. Phys. Chem. A* **1998**, *102*, 5775. (c) Richert, R.; Richert, M. *Phys. Rev. E* **1998**, *58*, 779. (d) Richert, R. *J. Chem. Phys.* **2000**, *113*, 8404.
(39) Yanagimachi, M.; Tamai, N.; Masuhara, H. *Chem. Phys. Lett.* **1992**, *200*, 469.
(40) (a) Pant, D.; Levinger, N. E. *Chem. Phys. Lett.* **1998**, *292*, 200. (b) Pant, D.; Levinger, N. E. *J. Phys. Chem. B* **1999**, *103*, 7846. (c) Pal, S. K.; Sukul, D.; Mandal, D.; Bhattacharyya, K. *J. Phys. Chem. B* **2000**, *104*, 2613.
(41) Shang, X.; Benderskii, A. V.; Eisenthal, K. B. *J. Phys. Chem. B* **2001**, *105*, 11578.
(42) (a) Nandi, N.; Bhattacharyya, K.; Bagchi, B. *Chem. Rev.* **2000**, *100*, 2013. (b) Bhattacharyya, K.; Bagchi, B. *J. Phys. Chem. A* **2000**, *104*, 10603. (c) Bhattacharyya, K. *J. Fluoresc.* **2001**, *11*, 167.
(43) Levinger, N. E. *Curr. Opin. Colloid Interface Sci.* **2000**, *5*, 118.
(44) Datta, A.; Das, S.; Mandal, D.; Pal, S. K.; Bhattacharyya, K. *Langmuir* **1997**, *13*, 6922.
(45) Sen, S.; Sukul, D.; Dutta, P.; Bhattacharyya, K. *J. Phys. Chem. B* **2002**, *106*, 3763.
(46) Shirota, H.; Castner, E. W., Jr. *J. Am. Chem. Soc.* **2001**, *123*, 12877.
(47) Lee, B. J.; Diken, E. L.; Wiewior, P. P.; Castner, E. W., Jr. Manuscript in preparation.

(48) Ratner, M. A.; Shriver, D. F. *Chem. Rev.* **1988**, *88*, 109.
(49) Bruce, P. G.; Vincent, C. A. *J. Chem. Soc., Faraday Trans.* **1993**, *89*, 3187.
(50) Reynolds, L.; Gardecki, J. A.; Frankland, S. J. V.; Horng, M. L.; Maroncelli, M. *J. Phys. Chem.* **1996**, *100*, 10337.
(51) Gardecki, J. A.; Maroncelli, M. *J. Phys. Chem. A* **1999**, *103*, 1187.
(52) *CRC Handbook of Chemistry and Physics*, 77th ed.; CRC Press: Boca Raton, FL, 1996.
(53) Berry, G. C.; Fox, T. G. *Adv. Polym. Sci.* **1968**, *5*, 261.
(54) Doi, M.; Edwards, S. F. *The Theory of Polymer Dynamics*; Oxford University Press: Oxford, 1986.
(55) Strobl, G. R. *The Physics of Polymers*, 2nd ed.; Springer: Berlin, 1997.
(56) Matsuoka, S. *Relaxation Phenomena in Polymars*; Carl Hanser Verlag: Munich, 1992.
(57) Horng, M. L.; Gardecki, J. A.; Maroncelli, M. *J. Phys. Chem. A* **1997**, *101*, 1030.
(58) Siano, D. B.; Metzler, D. E. *J. Chem. Phys.* **1969**, *51*, 1856.
(59) Edwards, J. T. *J. Chem. Educ.* **1970**, *47*, 261.
(60) van der Zwan, G.; Hynes, J. T. *J. Phys. Chem.* **1985**, *89*, 4181.
(61) Dote, J. L.; Kivelson, D.; Schwartz, R. N. *J. Phys. Chem.* **1981**, *85*, 2169.
(62) Fleming, G. R. *Chemical Applications of Ultrafast Spectroscopy*; Oxford University Press: New York, 1986.
(63) Sluch, M. I.; Somoza, M. M.; Berg, M. A. *J. Phys. Chem. B* **2002**, *106*, 7385.
(64) Moog, R. S.; Bankert, D. L.; Maroncelli, M. *J. Phys. Chem.* **1993**, *97*, 1496.
(65) Nibbering, E. T. J.; Tschirschwitz, F.; Chudoba, C.; Elsaesser, T. *J. Phys. Chem. A* **2000**, *104*, 4236.
(66) Cave, R. J.; Burke, K.; Castner, E. W., Jr. *J. Phys. Chem. A* **2002**, *106*, 9294.
(67) Fee, R. S.; Maroncelli, M. *Chem. Phys.* **1994**, *183*, 235.
(68) Argaman, R.; Huppert, D. *J. Phys. Chem. A* **1998**, *102*, 6215.
(69) Lin, Y.-H.; Wang, C. H. *J. Chem. Phys.* **1978**, *69*, 1546.
(70) Wang, C. H.; Lin, Y.-H.; Jones, D. R. *Mol. Phys.* **1979**, *37*, 287.
(71) Wang, C. H.; Li, B. Y.; Rendell, R. W.; Ngai, K. L. *J. Non-Cryst. Solids* **1991**, *131*−*133*, 870.
(72) Noudou, T.; Matsuoka, T.; Koda, S.; Nomura, H. *Jpn. J. Appl. Phys.* **1996**, *35*, 2944.
(73) Kaatze, U.; Kettler, M.; Pottel, R. *J. Phys. Chem.* **1996**, *100*, 2360.
(74) Sato, T.; Niwa, H.; Chiba, A.; Nozaki, R. *J. Chem. Phys.* **1998**, *108*, 4138.
(75) Olender, R.; Nitzan, A. *J. Chem. Phys.* **1995**, *102*, 7180.
(76) Flory, P. J. *Principles of Polymer Chemistry*; Cornell University Press: Ithaca, NY, 1953.
(77) de Gennes, P. D. *Scaling Concepts in Polymer Physics*; Cornell University Press: Ithaca, NY, 1979.
(78) Graessley, W. W. *Adv. Polym. Sci.* **1974**, *16*, 1.
(79) Rouse, P. E. *J. Chem. Phys.* **1953**, *21*, 1272.
(80) Shi, J.; Vincent, C. A. *Solid State Ionics* **1993**, *60*, 121.
(81) Borodin, O.; Smith, G. D. *Macromolecules* **2000**, *33*, 2273.
(82) Maroncelli, M.; Fleming, G. R. *J. Chem. Phys.* **1987**, *86*, 6221.